Electrostatic Interactions in Ubiquitin: Stabilization of Carboxylates by Lysine Amino Groups†

Monica Sundd,‡ Nicole Iverson,‡ Beatriz Ibarra-Molero,§ Jose M. Sanchez-Ruiz,§ and Andrew D. Robertson*,‡

Department of Biochemistry, University of Iowa College of Medicine, Iowa City, Iowa 52242, and Departamento de Quimica Fisica, Facultad de Ciencias, Universidad de Granada, 18071 Granada, Spain

Received January 22, 2002; Revised Manuscript Received April 24, 2002

ABSTRACT: To explore electrostatic interactions in ubiquitin, pK_a values have been determined by NMR for all 12 carboxyl groups in wild-type ubiquitin and in variants where single lysines have been replaced by neutral residues. Aspartate pK_a values in ubiquitin range from 3.1 to 3.8 and are generally less than model compound values. Most aspartate pK_a values are within 0.2 pH unit of those predicted with a simple Tanford−Kirkwood model. Glutamate pK_a values range from 3.8 to 4.5, close to model compound values and differing by 0.1−0.8 pH unit from calculated values. To determine the role of positive charges in modulating carboxyl pK_a values, we mutated lysines at positions 11, 29, and 33 to glutamine and threonine. NMR studies with these six single-site mutants reveal significant interactions of Lys 11 and Lys 29 with Glu 34 and Asp 21, respectively: pK_a values for Glu 34 and Asp 21 increase by approximately 0.5−0.8 pH unit, similar to predicted values, when the lysines are replaced by neutral residues. In contrast, the predicted interaction between Lys 33 and Glu 34 is not observed experimentally. In some instances, substitution of lysine by glutamine and threonine did not lead to the same changes in carboxyl pK_a values. These may reflect new short-range interactions between the mutated residues and the carboxyl groups. Carboxyl pK_a shifts > 0.5 pH unit result from mutations at groups that are <5 Å from the carboxyl group. No interactions are observed at >10 Å.

Electrostatic interactions in proteins have long been a subject of considerable interest because of the long distances over which they exert their influence (*1*, *2*) and their role in stability (*3*, *4*), solubility (*5*), catalysis (*6*−*11*), ligand binding (*12*, *13*), and redox potentials (*6*, *14*−*16*). Numerous efforts have been directed toward a more precise and complete understanding of the molecular basis for these interactions in proteins. Experimental determination of ionization equilibria is one approach to gather information about charge−charge interactions. In this regard, multiple pK_a values for many proteins have been determined by 2D NMR (e.g., *17*−*25*). This approach is particularly fruitful because these pK_a values are the only opportunity to observe experimentally the energetics of electrostatic interactions at multiple residues simultaneously.

Major advances toward understanding electrostatic interactions in proteins are being made in the area of theory. The various electrostatic models differ primarily at the level of molecular detail with which the protein and solvent are treated (*26*−*33*). Relatively simple treatments based on the Tanford−Kirkwood model (*34*) can yield good agreement between most calculated and observed pK_a values in proteins (*35*−*37*). However, most ionizable groups are exposed to solvent and most observed pK_a values are within 1 unit of model compound values (*29*, *33*, *38*, *39*). For these groups, the small pK_a perturbations are probably dominated by charge−charge interactions through solvent. Consequently, knowledge of distances between charges and use of a relatively high dielectric constant are sufficient to capture the relevant molecular detail. Some investigators argue that most pK_a values are not discriminative benchmarks for comparison with theory and that the focus, at least as far as benchmarks are concerned, should be on the small subset of pK_a values that differ by more than 2 units from model compound values (*33*). Such pK_a values are found primarily on buried and partially buried groups. For reasonable agreement between calculated and experimental pK_a values at these groups to be achieved, protein and solvent must be treated in more molecular detail (*33*, *40*).

The level of agreement between experimental and theoretical pK_a values is most often expressed as root-mean-square error, RMS, and efforts to refine electrostatic models generally aim to minimize the overall RMS (*29*, *36*). Because they are usually averages over many ionizable groups, RMS values tend to obscure the small but significant number of outlying groups, present in most proteins, where the level of agreement between experiment and theory is poor even for solvent-exposed residues. In these cases, intercharge

† The work was supported by NIH Grant GM46869 to A.D.R and Grant BIO2000-1437 from the Spanish Ministry of Science and Technology to J.M.S-R.

* Corresponding author. Tel: (319) 335-6515. Fax: (319) 335-9570. E-mail: andy-robertson@uiowa.edu.

‡ University of Iowa College of Medicine.

§ Universidad de Granada.

[1] Abbreviations: EDTA, ethylaminediaminetetraacetic acid; DTT, dithiothreitol; OD_{600}, apparent absorbance at 600 nm; IPTG, isopropyl-β-D-thiogalactoside; MALDI-TOF, matrix-assisted-laser-desorption-ionization-time of-flight; NMR, nuclear magnetic resonance; SDS−PAGE, sodium dodecyl sulphate polyacrylamide gel electrophoresis; TOCSY, total correlation spectroscopy; TSP, sodium-3-(trimethylsilyl)-propionate-2, 2,3,3-d 4.

10.1021/bi025571d CCC: $22.00
Published on Web 05/23/2002

distances determined in X-ray or NMR structures and the use of a high dielectric constant are not sufficient for accurate prediction of pK_a values. The discrepancies may arise from uncertainties in the molecular models or from errors in the theory, but unfortunately, most studies lack the information needed to discriminate between these possibilities.

More precise experimental data regarding the molecular basis for pK_a values in proteins can be obtained when pK_a determinations are combined with site-directed mutagenesis (*24*, *41*, *42*, and references therin). The role of specific residues in perturbing pK_a values can be identified by substitution of wild-type charged residues with neutral residues or residues of opposite charge and subsequent pK_a determinations by NMR. Moreover, concomitant analysis of these results and those predicted by theory should be an excellent way to evaluate and refine the models more precisely.

The present study focuses on the molecular basis for the ionization behavior of the 12 carboxyl groups in ubiquitin. Ubiquitin is particularly well suited for investigation of ionization equilibria and electrostatic interactions because of its small size, known structure (*43*), stability to extremes of pH and temperature (*44*, *45*), and complete proton NMR assignments (*46*, *47*). The present work is partly inspired by and complements previous studies investigating the role of ionizable residues in the stability and solubility of ubiquitin (*48*−*50*). The pK_a values for the carboxyl groups in wild-type ubiquitin are reported and compared to pK_a values in single-site variants in which lysines have been replaced by neutral residues. These results are compared with those predicted using a modified Tanford−Kirkwood model that has been successful in predicting the effects of mutations at charged residues on the stability of ubiquitin (*49*). This model incorporates solvent-accessibility factors for ionizable groups and is based on the model originally proposed by Gurd and co-workers (*51*, *52*).

MATERIALS AND METHODS

Materials. Wild-type bovine ubiquitin was purchased from Sigma Chemical Co. (St. Louis, MO) and dialyzed three times against deionized distilled water before use. Oligonucleotide primers were purchased from Integrated DNA Technologies (Coralville, IA). Competent *Escherichia coli* BL21 (DE3) cells were purchased from Novagen Inc. (Madison, WI). Deuterium oxide (99.9 atom % D), and sodium 3-(trimethylsilyl)-propionate-2, 2,3,3-d_4 (98 atom % D) were obtained from Cambridge Isotope Laboratories (Cambridge, MA). Potassium chloride, IPTG and standard buffers at pH 2, 4, and 7 were from Fisher Scientific (Chicago, IL). NMR tubes (535-PP) were obtained from Wilmad (Buena, NJ). All other chemicals were the best available reagant grade.

Mutagenesis and Protein Purification. Ubiquitin mutants were constructed using the plasmid pRSUb (*53*) and QuikChange site-directed mutagenesis kit from Stratagene (La Jolla, CA). Mutant codons were located in the middle of mutagenic primers which consisted of no more than 45 nucleotides. The mutations were confirmed by DNA sequencing of the coding regions in the resulting plasmids; sequencing was performed by the University of Iowa DNA Facility.

Proteins were expressed in *E. coli* BL21 (DE3) cells. Cells were grown at 37 °C to an OD_{600} of 1.0 in Luria Broth supplemented with 100 μg/mL ampicillin, and protein expression was then induced with 0.5 mM IPTG. After 3 h, cells were pelleted by centrifugation and stored overnight at −20 °C. Frozen pellets were thawed, dissolved in 0.05 M Tris-HCl containing 0.5 mM EDTA and 1mM DTT, and then lysed by sonication. After centrifugation at 9000 g for 20 min, most of the proteins in ice-cold supernatant were precipitated by dropwise addition of perchloric acid to a final volume of 5% (v/v). After centrifugation at 9000 g for 20 min, the supernatant was dialyzed against 0.05 M ammonium acetate buffer, pH 4.5. Pure ubiquitin was obtained by cation-exchange chromatography on a CM-52 column (1 × 10 cm) equilibrated with 0.05 M ammonium acetate buffer, pH 4.5. Unbound protein was removed by washing the column with the same buffer, and ubiquitin was eluted with 0.1 M ammonium acetate, pH 5.5. The purity of the fractions was assessed by SDS−PAGE. Pooled fractions containing ubiquitin were dialyzed at 4 °C against three changes of deionized distilled water, lyophilized, and stored at −20 °C. Typical yields of pure protein were 75−100 mg per liter of cell culture. Mutations in the proteins were confirmed by amino acid analysis and MALDI-TOF performed at the Molecular Analysis Facility, The University of Iowa College of Medicine, and by 2D NMR as described below.

NMR Sample Preparation. A 2 mM solution of ubiquitin was prepared by dissolving lyophilized protein in 0.1 M KCl containing 0.5 mM TSP and 10% D_2O (v/v). TSP was used as an internal standard for chemical shift. The pH of the solution was adjusted with concentrated HCl and KOH at 25 °C and measured with a Model 611 Orion Research pH meter equipped with a 3 mm glass electrode (Mettler Toledo, Columbus, OH). The pH of the sample was measured before and after the acquisition of NMR spectrum at each titration point. In all the cases, variation in the pH measured before and after the acquisition was less than 0.05 pH unit, and an average of the two values was used for data analysis. The reported pH values were not corrected for the deuterium isotope effect on the glass electrode.

NMR Spectroscopy. TOCSY data (*54*) were acquired on a Varian INOVA 500 spectrometer located in the University of Iowa College of Medicine NMR Facility. Sample volumes were 650 μL. The carrier frequency was set on the water signal, and solvent suppression was achieved by continuous-wave irradiation of the solvent resonance during the 1.5 s relaxation delay. TOCSY experiments consisted of 256 t_1 increments, each of which consisted of four transients and 2048 time-domain points. The spectral width in both dimensions was 6000 Hz and the mixing time was 100 ms. Temperature in the probe was calibrated using methanol as the standard (*55*).

Processing of the NMR data was carried out using the Varian software. The time domain data were weighted using an unshifted Gaussian filter in the f_2 dimension and a sine bell in the f_1 dimension prior to Fourier transformation; the time constants were 0.132 and 0.075 s, respectively, in the two dimensions. The final digital resolution was 2.92 Hz/point in both dimensions, and the estimated uncertainties in chemical shifts were 0.006 and 0.05 ppm in ω_2 and ω_1 dimensions, respectively.

pK_a Determinations. Apparent pK_a values for carboxyl groups were obtained by fitting proton chemical shifts versus pH to the following modified Hill equation (*23*, *24*):

$$\delta_{obs} = \delta_A[1 + 10^{n(pK_a - pH)}]^{-1} + \delta_{HA}[1 - (1 + 10^{n(pK_a - pH)})^{-1}] \quad (1)$$

where δ_{obs} is the observed chemical shift at a given pH, δ_A and δ_{HA} are the chemical shifts of fully deprotonated and protonated species, respectively, and n is the Hill coefficient, a measure of cooperativity. Nonlinear least-squares analysis was done using KaleidaGraph™ version 3.08 (Synergy Software, Reading, PA).

Chemical shifts were referenced with respect to TSP (*56*, *57*), and chemical shift data were corrected for the pH dependence of TSP using the equation

$$\delta_{corr} = (\delta_{obs} - 0.019)\,(1 + 10^{(5 - pH)})^{-1} \quad (2)$$

The proton chemical shifts at 30 °C and pH 5.5 were identified on the basis of resonance assignments made under similar conditions (*46*, *47*).

pK_a Calculations. The pK_a values were calculated using the Tanford−Kirkwood model (*34*) with Bashford−Karplus reduced-set-of-sites approximation (*27*) as described previously (*48*). This simple approach, referred to here as the TK−BK model, treats the native protein as a low-dielectric-constant sphere surrounded by a high-dielectric-constant solution and places the charges on the surface of the sphere according to the pair wise distances taken from the crystal structure (*43*) (PDB file 1ubq). Charges were placed on the following atoms: Cγ of aspartate; Cδ of glutamate; Cϵ of histidine; Nζ of lysine; Cζ of arginine; and the α-carboxyl carbon and α-amino nitrogen of Gly 76 and Met 1, respectively. Hill coefficients, n, derived from the TK−BK model were calculated by fitting the pH dependence of the predicted fraction carboxylate ion, X, to the following equation:

$$X = (1 + 10^{n(pK_a - pH)})^{-1} \quad (3)$$

RESULTS

Accurate pK_a determinations in native ubiquitin are predicated on its remaining folded at acidic pH. All indications from the TOCSY data are that ubiquitin is folded at pH 1.0 and that the structure is very similar to that at pH 6. $C_\alpha H$ resonances are especially good indicators of secondary structure (*58*). Sixty-five of the 76 possible $C_\alpha H$ resonances can be assigned at acidic pH, and all but two showed chemical shifts that are within 0.15 ppm of the values at pH 6 (data not shown). Of the two $C_\alpha H$ showing larger changes, the 0.27 ppm difference at the C-terminal Gly 76 can be explained by the titration of its α-carboxyl group (Figure 1; Table 1), and the pH dependence of the 0.30 ppm shift for Glu 64 $C_\alpha H$ is consistent with titration of its own side chain. The observation that ubiquitin is folded at acidic pH at 30 °C is consistent with previous results for mammalian ubiquitin (all ubiquitins from mammals have identical sequences) and the closely related yeast ubiquitin (*44*, *48*, *59*).

Carboxyl pK_a Values in Wild-Type Ubiquitin. The pH dependent changes in ^{1}H chemical shifts of carboxyl-containing residues in wild-type ubiquitin in 0.1 M KCl were monitored in a series of TOCSY spectra recorded at 0.5 unit intervals from pH 1.0 to 7.0. The ^{1}H resonance assignments used in this study are consistent with both of the published studies, except in the cases of Asp 21 and Asp 52 where the published assignments are in disagreement (*46*, *47*). The titration studies confirm the $C_\beta H$ assignments for Asp 21 made by Weber and co-workers (*47*) and for Asp 52 made by Di Stefano and Wand (*46*). The spin system assigned to Asp 52 by Weber and co-workers is probably Asn 60 and vice versa.

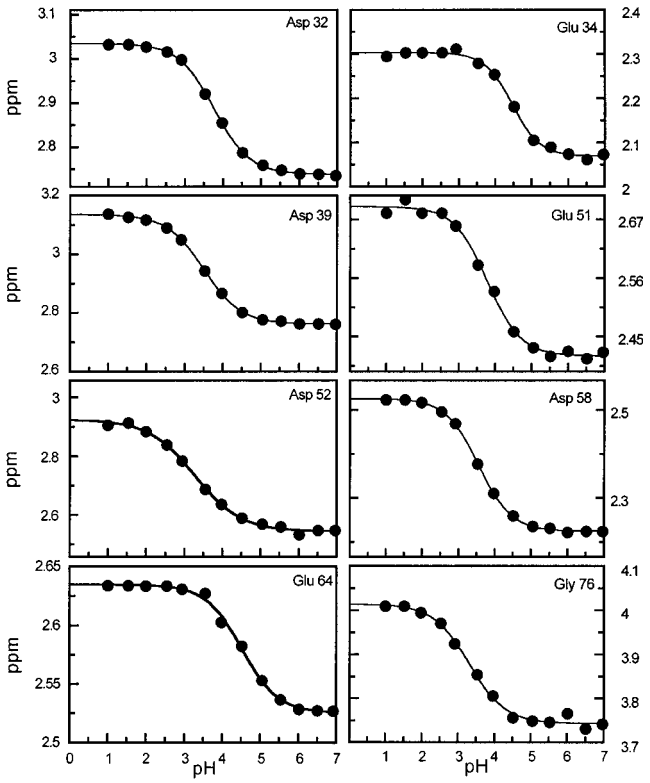

FIGURE 1: pH dependences of the chemical shifts for resonances in the carboxyl-containing residues of wild-type ubiquitin at 30 °C. Samples consisted of 2 mM protein in 0.1M KCl, 10% D_2O, and 0.5 mM TSP. The fits to eq 1 are shown in solid lines.

The principal resonances for most pK_a determinations were for protons nearest the ionizing carboxyl groups: $C_\beta H$ in aspartates, $C_\gamma H$ in glutamates, and $C_\alpha H$ in Gly 76, the C-terminal residue. The one exception is Glu 64, where the $C_\beta H$ resonances were monitored. As illustrated in Figure 1 and reported in Table 1, these resonances show downfield chemical shift changes ranging from 0.11 to 0.44 ppm with decreasing pH. Most of the pH dependences are consistent with simple titrations, with Hill coefficients close to 1.0 (Table 1). However, the pH dependences for Glu 24, Asp 21, Asp 52, and, possibly, Glu 18 are broadened significantly, as evidenced by Hill coefficients of 0.7−0.8. The broad transitions probably reflect the influence of nearby carboxyl groups that are titrating over the same range of pH.

Comparison with Theoretical Values. Theoretical and experimental pK_a values show very good agreement at four of the five aspartates, with differences ranging from zero at Asp 39 to 0.2 unit at Asp 52 (Table 1). Calculated pK_a values for Asp 21 and the C-terminal Gly 76 are 0.4 and 0.3 units greater, respectively, than the experimental values. At glutamate residues, theoretical and experimental pK_a values

Table 1: Carboxyl pK_a Values in Wild-Type Ubiquitin in 0.1 M KCl and at 30 °C

residue	^{1}H[a]	δ_A[b]	$\Delta\delta$[c]	pK_{exp}[d]	pK_{pred}[e]	Hill n_{exp}[f]	Hill n_{pred}[g]	mol. surf.[h]	SA[i]
Glu 16	C_γH	2.09	−0.36	3.9	4.2	1.1	0.9	19.0	0.88
Glu 18	C_γH	2.32	−0.22	4.3	4.2	0.8	0.9	14.2	0.69
Asp 21	C_βH	2.49	−0.30	3.1	3.5	0.7	0.8	7.1	0.24
Glu 24	C_γH	2.36	−0.24	4.3	4.6	0.7	0.9	18.4	0.77
Asp 32	C_βH	2.73	−0.30	3.8	3.9	0.9	1.0	18.1	0.82
Glu 34	C_γH	2.07	−0.23	4.5	3.7	1.1	0.9	7.1	0.23
Asp 39	C_βH	2.76	−0.38	3.6	3.6	0.9	1.0	7.6	0.61
Glu 51	C_γH	2.41	−0.28	3.8	4.4	0.9	0.9	18.2	0.77
Asp 52	C_βH	2.61	−0.44	3.4	3.2	0.7	0.9	8.5	0.49
Asp 58	C_βH	2.27	−0.29	3.6	3.7	1.0	0.9	8.0	0.37
Glu 64	C_βH	2.52	−0.11	4.5	4.2	0.9	1.0	12.0	0.56
Gly 76	C_αH	3.74	−0.27	3.3	3.6	0.9	1.0	19.3	1.00
Ile 13	NH	9.55	0.32	4.4	-	0.9	-	-	-
Glu 18	NH	8.68	1.36	2.9	-	0.9	-	-	-
Ser 20	NH	7.04	−0.17	3.2	-	0.7	-	-	-
Asn 25	N_δH	7.85	0.32	3.1	-	0.6	-	-	-
Thr 55	NH	8.77	1.25	3.5	-	1.3	-	-	-

[a] Resonance used to determine pK_a values. [b] Chemical shift for deprotonated species; δ_A in eq 1. [c] Fitted amplitude of the pH-dependent change in chemical shift from eq 1: $\Delta\delta = \delta_A - \delta_{HA}$. [d] p$K_a$ value derived from fits to eq 1. Standard deviations of the fits were ≤0.1. [e] pK_a values predicted by the Tanford−Kirkwood model as described in Materials and Methods. The intrinsic pK_a values used in these calculations are 4.0 and 4.5 for aspartate and glutamate, respectively. [f] Hill coefficient derived from fits to eq 1. Standard deviations of the fits were ≤ 0.1. [g] Hill coefficient predicted by the Tanford−Kirkwood model as described in Materials and Methods. [h] Total van der Waals surface, in Å^2, of the carboxyl oxygen atoms that is accessible to solvent. Surface areas were calculated with the WHAT IF program (74). [i] Normalized solvent-accessibility (SA) parameter used for calculations with the modified Tanford−Kirkwood model (48). This is the SA value for the side chain atoms of residue X in ubiquitin relative to the same side chain in a Gly−X−Gly tripeptide.

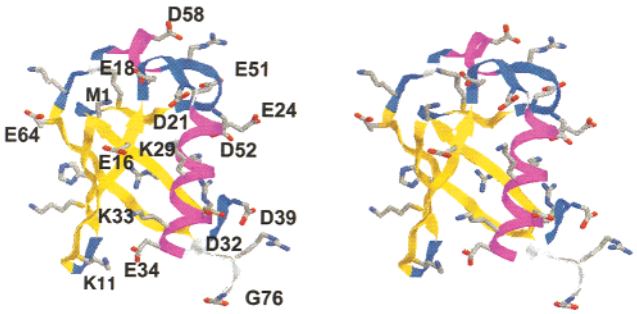

FIGURE 2: Ribbon diagram based on the X-ray structure of mammalian ubiquitin (43; PDB file 1ubq). All acidic and basic residues are shown as sticks. All acidic residues and the three mutated lysine residues are labeled with the one letter amino acid code. The figure was generated with RasMol (version 2.7.2.1; Bernstein and Sons, www.bernstein-plus-sons.com).

differ by only 0.1 unit at Glu 18 and 0.3 unit at Glu 16, Glu 24, and Glu 64, and they show differences of 0.8 and 0.6 units at Glu 34 and Glu 51 (Table 1). Eight of the 12 predicted Hill coefficients are within 0.1 unit, and all are within 0.2 unit, of experimental values.

pH Dependence of Amide Proton Resonances. Hydrogen bonds between carboxyl groups and backbone amide protons give rise to large upfield changes in NH chemical shift upon protonation of the carboxyl groups (*60*, *61*). On the basis of the crystal structure of ubiquitin (Figures 2 and 3), we hypothesized that the amide protons of Glu 18 and Thr 55 are hydrogen bonded to the carboxyl groups of Asp 21 and Asp 58, respectively, and that the chemical shifts of Glu 18 NH and Thr 55 NH would show the expected pH dependences. The data for Glu 18 NH and Thr 55 NH are consistent with this hypothesis: the chemical shift changes are >1 ppm, and the apparent pK_a values match those for the carboxyl group accepting the putative hydrogen bond (Table 1; Figure 4B; data not shown). Moreover, changes in the pK_a for Asp 21 induced by mutation are also manifested in the pH dependence for Glu 18 NH (Figure 4B; see below).

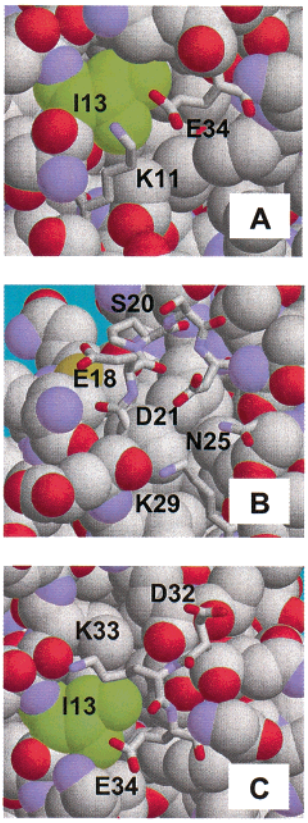

FIGURE 3: Molecular environment near (top) Lys 11, (middle) Lys 29, and (bottom) Lys 33 in the X-ray structure of mammalian ubiquitin (43; PDB file 1ubq). Residues discussed in the text are labeled with the one letter amino acid code. The figure was generated with RasMol (version 2.7.2.1; Bernstein and Sons, www.bernstein-plus-sons.com).

Significant pH dependences were observed at a few other NH resonances as well. A 0.32 ppm chemical shift change was observed at one of the side chain amide protons of Asn 25, and the pH dependence matches the pK_a for Asp 21

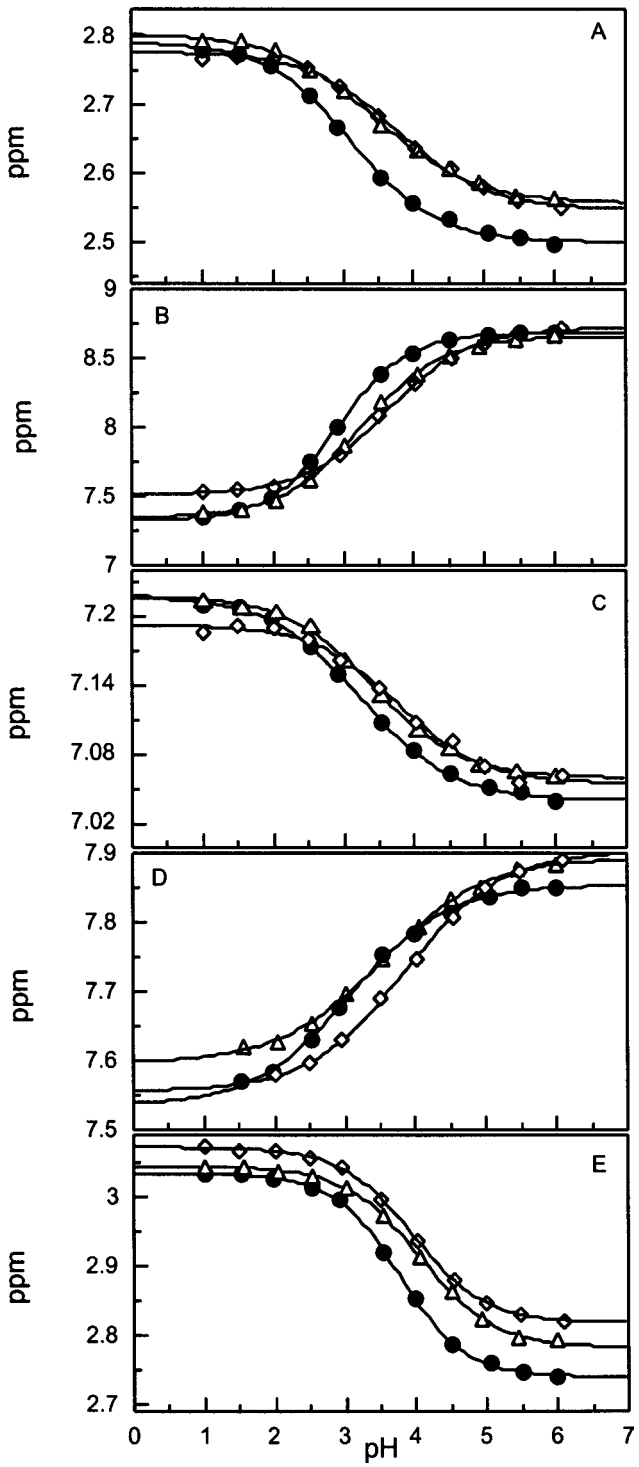

FIGURE 4: pH-induced chemical shift changes at 30 °C for (A) $C_\beta H$ of Asp 21, (B) NH of Glu 18, (C) NH of Ser 20, (D) $N_\delta H$ of Asn 25, and (E) $C_\beta H$ of Asp 32 in wild-type ubiquitin (●) and the two Lys 29 mutants, K29Q (△) and K29T (◇). The fits to eq 1 are indicated by the lines and the fitted parameters are reported in Table 3.

(Table 1; Figure 4D). The side chain oxygen and nitrogen atoms of Asp 21 and Asn 25, respectively, are separated by only 3.4 Å in the crystal structure (Figure 3B), although the geometry is not optimal for hydrogen bonding. However, the relative orientation of these two side chains varies in other structures of ubiquitin, with interatomic distances as short as 2.8 Å in a recent structure of tetrameric ubiquitin (*62*). We hypothesize that the side chains of Asp 21 and Asn 25 are indeed involved in some degree of hydrogen bonding in solution.

Of the remaining 61 backbone NH resonances in wild-type ubiquitin that could be identified at the extremes of pH, 55 had chemical shifts at acidic pH that were within 0.2 ppm of values at neutral pH (data not shown), consistent with conservation of the overall backbone structure at acidic pH (*58*). Among the six other NH resonances, pH dependences for all but Leu 71 can be explained by proximity to titrating carboxyl groups. The pH dependences for Glu 16 NH, Asp 39 NH, and Gly 76 NH reflect titration of their own carboxyl groups. Titration of Asp 39 also appears to be responsible for the pH dependence at Gln 40 NH. The pH dependence at Ile 13 NH is consistent with titration of the neighboring carboxyl group on Glu 34 (Table 1; Figures 3C and 5B), and this is confirmed in studies of mutants described below. Ala 28 NH and Leu 71 NH show pH dependences with amplitudes of 0.34 and 0.23 ppm, respectively, and apparent pK_a values of 4.3−4.4. The change at Ala 28 NH is probably due to titrations of Glu 24, which is 7.7 Å from Ala 28 NH in the crystal structure and has a similar Hill coefficient and apparent pK_a value (Table 1). The pH dependence for Leu 71 NH is a mystery: Glu 34 is the nearest residue, with a pK_a near 4.4, but its carboxyl group is 13 Å away from Leu 71 NH. A small amplitude change in Ser 20 NH chemical shift reports the titration of Asp 21 (Table 1; Figure 4C; see below).

Mutagenesis Studies. Many of the carboxyl pK_a values in wild-type ubiquitin are less than values for model compounds, and none of the observed pK_a values are significantly greater than model compound values (Table 1). The decreased pK_a values suggest that the structure of ubiquitin stabilizes negative charges on the carboxyl groups. One hypothesis to explain stabilization of a negative charge is the presence of positively charged groups nearby.

To determine the extent to which positively charged groups in ubiquitin are interacting with the carboxyl groups, we made six single-site mutants in which lysines at positions 11, 29, and 33 were replaced by threonine and glutamine and all 12 carboxyl pK_a values were determined in each mutant. The rationale for substituting with threonine and glutamine is similar to that described previously for studies of ovomucoid third domain (*24*): these substitutions are commonly observed in sequences for ubiquitin-like proteins, they typically represent single base changes, and the use of two different side chains facilitates distinguishing between general effects due to charge-neutralization and more specific effects due, for example, to formation of new local interactions in the variant proteins. Lysines 11, 29, and 33 were chosen because of their proximity to carboxyl groups in the crystal structure (Figures 2 and 3; Table 2). The NMR spectra for all mutants were very similar to spectra for wild-type, with the exception of differences seen at the sites of mutation. The overall structures for the mutants are thus similar to the structure of wild-type ubiquitin.

Interactions of Lys 11. Lysine 11 is in the second strand of β-sheet, and in the crystal structure, its ϵ-amino group is 3.3 Å from the closest carboxyl oxygen in Glu 34, located at the C-terminus of the major helix (Figures 2 and 3A; Table 2). The proximity of these side chains is the principal basis for predicting a low pK_a of 3.7 for Glu 34 in wild-type ubiquitin (Table 1), so the observed pK_a of 4.5 in wild-type

Table 2: Distances between Mutated Residues and the Nearest Carboxylates in Ubiquitin[a]

res. no.	Glu 16	Glu 18	Asp 21	Asp 32	Glu 34
Lys 11	15.2	21.7	18.9	13.5	3.3
Lys 29	7.1	8.4	4.9	8.5	12.9
Lys 33	8.5	15.3	13.3	8.7	5.6

[a] Distances in angströms between the mutated lysine residues and the nearest acidic residues, as measured in the X-ray structure of ubiquitin (PDB file 1ubq) using Sybyl (Tripos Associates, St. Louis, MO). The distances are between the Nϵ of lysine and the nearest carboxyl oxygen on the indicated acidic residue.

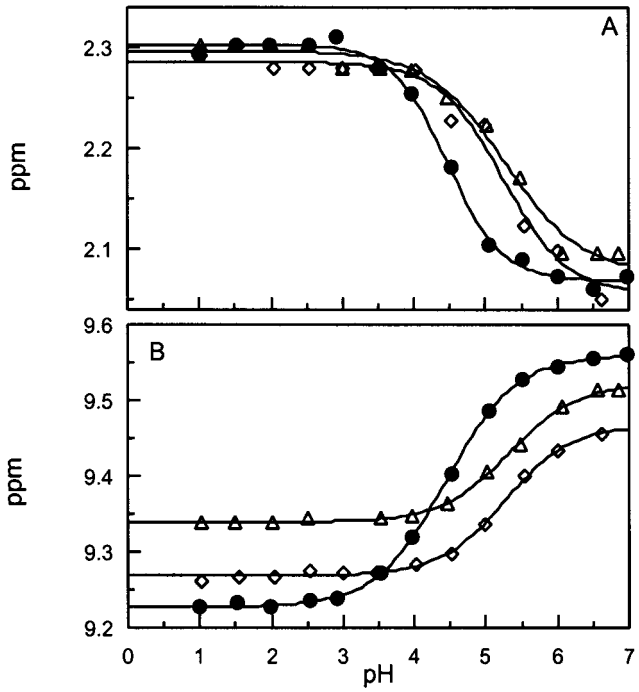

FIGURE 5: pH-induced chemical shift changes at 30 °C for the (A) $C_\gamma H$ and (B) NH resonances of Glu 34 and Ile 13, respectively, in wild-type ubiquitin (●) and the two Lys 11 mutants, K11Q (△) and K11T (◇). The fits to eq 1 are indicated by the lines and the fitted parameters are reported in Table 3.

ubiquitin is surprising. However, the fact that Lys 11 is indeed interacting significantly with Glu 34 is demonstrated clearly by substitutions at position 11: in K11Q and K11T, the pK_a of Glu 34 is about 0.8 unit greater than the wild-type value (Figure 5A; Table 3). This change agrees fairly well with that predicted by the TK−BK model (Table 3). The pH dependence for Ile 13 NH reports a similar change in pK_a, confirming that this resonance is indeed reporting on the pK_a of Glu 34 (Figure 5B). As predicted, the eleven other carboxyl groups shows pK_a changes $\leq$0.2 unit, which is consistent with the relatively large distances between these groups and Lys 11 (Table 2).

Interactions of Lys 29. Lys 29 is in the major helix, and its ϵ-amino group is 4.9 Å from the nearest carboxyl oxygen of Asp 21, which is located in the turn connecting the alpha helix to strand 2 of the β-sheet (Figures 2 and 3B; Table 2). The side chain amino group of Lys 29 is also about 8 Å from the carboxyl groups of Glu 16, Glu 18, and Asp 32. Mutation of Lys 29 to glutamine and threonine leads to increased pK_a values at Asp 21, as predicted with the TK−BK model, but the magnitude of the change in K29Q and K29T is different, 0.4 and 0.7, respectively (Figure 4A; Table 3). The changes at Asp 21 are mirrored at Glu 18 NH, Ser 20 NH, and Asn 25 $N_\delta H$ (Figures 4B−D), confirming that these resonances are indeed reporting the pK_a of Asp 21 and that the two mutations give rise to significantly different pK_a changes. These observed pK_a changes are similar to the 0.4 unit increase predicted with the TK−BK model. An increase of about 0.2−0.3 pH unit is also observed at Asp 32 in K29Q and K29T, but little or no change is observed at either Glu 16 or Glu 18 (Figure 4; Table 3; data not shown).

Table 3: Carboxyl pK_a Values for Selected Residues in Ubiquitin Variants in 0.1 M KCl, 30 °C[a]

mutation[b]	residue	^{1}H[c]	δ_A[d]	p$K_{a,mut}$[e]	Δp$K_{a,exp}$[f]	Δp$K_{a,pred}$[g]
K11 Q/T	Glu 18	$C_\gamma H$	2.31/2.32	4.4/4.1	+0.1/−0.2	0.0
	Glu 34	$C_\gamma H$	2.08/2.06	5.3/5.2	+0.8/+0.8	+0.5
	Ile 13	NH	9.52/9.46	5.3/5.2	+0.9/+0.8	+0.5
	Asn 25	$N_\delta H$	7.85/7.85	2.9/2.9	−0.2/−0.2	0.0
K29 Q/T	Glu 18	$C_\gamma H$	2.35/2.35	4.4/4.4	+0.1/+0.1	+0.1
	Asp 21	$C_\beta H$	2.56/2.55	3.5/3.8	+0.4/+0.7	+0.4
	Asp 32	$C_\beta H$	2.78/2.81	4.1/4.0	+0.3/+0.2	+0.1
	Glu 34	$C_\gamma H$	2.04/2.04	4.5/4.3	+0.1/+0.2	+0.0
	Ile 13	NH	9.58/9.56	4.5/4.5	+0.1/+0.1	+0.0
	Glu 18	NH	8.65/8.72	3.3/3.6	+0.3/+0.7	+0.4
	Ser 20	NH	7.06/7.05	3.4/3.8	+0.2/+0.5	+0.4
	Asn 25	$N_\delta H$	7.89/7.90	3.5/3.9	+0.5/+0.8	+0.4
K33 Q/T	Glu 16	$C_\gamma H$	2.09/2.06	3.9/3.9	−0.1/0.0	+0.1
	Asp 21	$C_\beta H$	2.50/2.50	3.0/3.0	−0.1/−0.1	+0.0
	Asp 32	$C_\beta H$	2.74/2.74	3.9/4.0	+0.1/+0.2	+0.1
	Glu 34	$C_\gamma H$	2.33/2.31	4.5/3.8	0.0/−0.7	+0.2
	Ile 13	NH	9.54/9.53	4.5/4.2	0.0/−0.3	+0.2
	Glu 18	NH	8.69/8.73	2.8/2.8	−0.1/−0.1	+0.0
	Ser 20	NH	7.04/7.04	3.2/3.1	0.0/−0.2	+0.0
	Asn 25	$N_\delta H$	7.86/7.87	2.9/3.0	−0.1/−0.1	+0.0

[a] Only residues with experimental or predicted nonzero pK_a changes are shown. [b] Throughout the table, entries to the left and right of the slash mark are for the glutamine and threonine variants, respectively. All Hill coefficients in variants were within 0.1 unit of wild-type values. [c] Resonances used to determine pK_a values. [d] Chemical shift for the deprotonated species; δ_A in eq 1. [e] pK_a values derived from fits to eq 2. Fitting errors were less than 0.15 in all the residues. [f] The observed change in pK_a upon mutation, Δp$K_{a,exp}$ = p$K_{a,mut}$ − p$K_{a,wt}$. [g] The predicted change in pK_a based on the TK−BK model.

The differences in pK_a values for Asp 21 in K29Q and K29T may not be immediately obvious from visual inspection of Figures 4A−C; the differences are more evident in the data for Asn 25 $N_\delta H$ (Figure 4D). However, the nonlinear least-squares fitting of the data in Figures 4A−C and error analysis strongly suggest that the differences in fitted pK_a values are statistically significant. With respect to least-squares analysis, a key difference in the data for K29Q and K29T is the plateau values for chemical shifts of Asp 21 $C_\beta H$ and Ser 20 NH at low pH (Figure 4A,C). These differences are systematic, not due to experimental error, and they are primarily responsible for the differences in the fitted pK_a values. In the case of Glu 18 NH, the total chemical shift change with varying pH is large, about 1.4 ppm, so the seemingly small difference in Figure 4B for the titration curves of K29Q and K29T is actually a large and statistically significant difference.

We have addressed the issue of experimental error by taking advantage of the seven independent experimental pK_a determinations made for this study. If we assume that carboxyl groups that are distant from the sites of mutation are not perturbed by the mutations, then the standard deviation of the mean pK_a values at these carboxyl groups will provide a reasonable estimate for experimental errors.

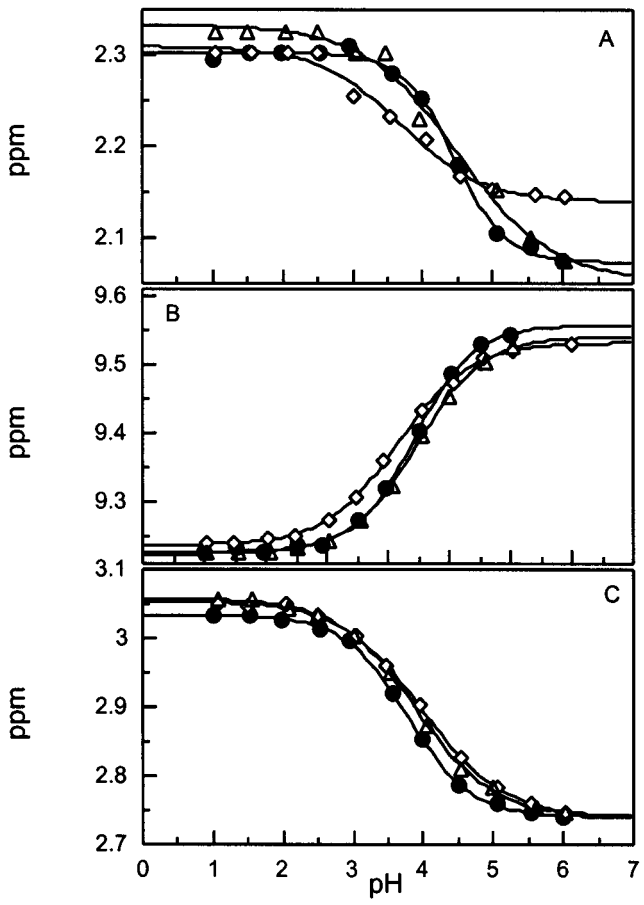

FIGURE 6: pH-induced chemical shift changes at 30 °C for the (A) $C_\gamma H$, (B) NH, and (C) $C_\beta H$ resonances of Glu 34, Ile 13, and Asp 32, respectively, in wild-type ubiquitin (●) and the two Lys 33 mutants, K33Q (△) and K33T (◇). The fits to eq 1 are indicated by the lines and the fitted parameters are reported in Table 3.

If the assumption is incorrect, then the resulting standard deviations will provide an overestimate for the true experimental error. We have used data for Asp 39, Glu 51, Asp 58, and Gly 76 for this analysis. These residues are far from the sites of mutation (Figure 1), and they show a range of pK_a values and amplitudes for chemical shift changes in wild-type ubiquitin (Table 1). The standard deviations about the mean pK_a values from the seven determinations range from 0.03 at Asp 58 to 0.10 at Gly 76 (data not shown), so a conservative estimate for the experimental error in pK_a determinations is 0.1 at the 67% confidence level.

Interactions of Lys 33. Lys 33 is located at about one turn C-terminal to Lys 29, and the ϵ-amino group of Lys 33 is only 5.6 Å from the nearest carboxyl oxygen of Glu 34 (Figures 2 and 3C; Table 2). Consequently, the TK−BK model suggests that mutation of Lys 33 to neutral residues should lead to a 0.2 unit increase in the pK_a for Glu 34, with smaller increases anticipated at a few other carboxyl groups (Table 3). A small increase is observed at Asp 32 in both K33Q and K33T (Figure 6C; Table 3). Surprisingly, however, the pK_a value for Glu 34 did not show any increases in K33Q and K33T, and in fact, the pK_a in K33T appears to decrease by 0.3−0.7 unit (Figure 6A,B; Table 3). Moreover, the decrease in pK_a observed at $C_\gamma H$ of Glu 34 appears to be greater than that observed in the pH dependence of Ile 13 NH (Figure 6A,B; Table 3), which usually reports the pK_a of Glu 34 (see above). Hill coefficients at both Glu 34 $C_\gamma H$ and Ile 13 NH show similar decreases in K33T relative to wild-type values, from about 1.0 to about 0.7 (Table 3). Overall, the results for K33T suggest that new and unanticipated interactions involving Glu 34 may have been introduced as a result of mutation.

DISCUSSION

The carboxyl pK_a values for wild-type ubiquitin in 0.1 M KCl range from 3.1 at Asp 21 to 4.5 at Glu 34 and Glu 64. The mean pK_a value for aspartate is 3.5 (± 0.3), and the mean value for glutamate is 4.2 (± 0.3). Similar distributions and mean values have been observed in other proteins (*29*, *38*). On average, the pK_a values for aspartate residues in ubiquitin are 0.4 unit below the smallest model compound value, while glutamate pK_a values are similar to model compound values (*63*). The structure of ubiquitin thus appears to stabilize negative charges on aspartates to a greater degree than on glutamates.

This trend is captured by the TK−BK model, which predicts that the mean pK_a values for aspartate and glutamate are 3.6 (± 0.2) and 4.2 (± 0.3), respectively. Similar observations have been made in other proteins by Antosiewicz and co-workers (*29*). However, pK_a predictions for aspartates in ubiquitin are more accurate than those for glutamates. The mean amplitude for the difference between predicted and observed pK_a for aspartates is 0.2 (± 0.1), and all but one of the predicted pK_a values are within 0.2 unit of experimental values. In contrast, the mean pK_a difference for glutamates is 0.4 (± 0.2), and all but one of the differences are >0.2 unit in magnitude. Antosiewicz and coworkers observed similar disagreement in the accuracy of pK_a predictions for aspartate versus glutamate (*29*). Interestingly, that study used a finite-difference Poisson−Boltzmann method to compute pK_a values, a different electrostatic model from the TK−BK procedure used in the present study. Possibly related observations were made in a recent survey of over 200 carboxyl pK_a values in proteins of known structure (*38*). Correlations between pK_a values and features of protein structure such as hydrogen bonding and calculated electrostatic potentials were detectable for aspartates but much less evident for glutamates. A possible explanation for the discrepancies between aspartate and glutamate may be differences in the accuracy and precision of aspartate and glutamate side chains in protein structures: uncertainties in positioning glutamate side chains are probably greater than those for the shorter aspartate side chains (*38*).

Carboxyl pK_a Values Near Model Compound Values. The observed pK_a values for Glu 16, Glu 18, Glu 24, Asp 32, Glu 64, and Gly 76 are within 0.3 unit of predicted values, similar to model compound values and the carboxyl groups for these residues are well exposed to solvent (Table 1). These groups are probably not interacting significantly with other groups in ubiquitin. This is partially confirmed for Glu 16, Glu 18, and Asp 32 by the mutagenesis experiments: the nearest lysine amino groups are more than 7 Å away (Table 2), and replacing these lysines with neutral residues has little or no effect on the pK_a values for Glu 16, Glu 18, and Asp 32 (Table 3). The observation that pK_a values for most of the solvent-exposed carboxyl groups in ubiquitin are similar to model compound values is consistent with results for a number of other proteins as well (*38*).

Perturbed Carboxyl pK_a Values. The moderately low pK_a values of 3.6 for the partially buried carboxyl groups of Asp 39 and Asp 58 are well predicted by the TK−BK model (Table 1). The slightly reduced pK_a at Asp 39 is primarily due to proximity of the guanidino groups on Arg 72 and Arg 74. Similarly, the carboxyl group of Asp 58 is only 3.9 Å from the guanidino group on Arg 54. Moreover, this carboxyl group is probably accepting a hydrogen bond from Thr 55 NH, as discussed previously.

Asp 21 has the lowest pK_a in ubiquitin, and both mutagenesis and electrostatics calculations indicate that Lys 29 is primarily responsible for this low pK_a (Table 3; Figures 4A−D). The pH dependences for NH chemical shifts suggest that the carboxyl group of Asp 21 may also be accepting hydrogen bonds from Glu 18 NH and the side chain amide protons of Asn 25. The picture is complicated a bit by the fact that K29Q and K29T yield different pK_a values at Asp 21, 3.5 and 3.8, respectively (Table 3). The reason for this difference is unclear. The ϵ-amino group of Lys 29 is 4.9 Å from the nearest carboxyl oxygen of Asp 21, so substitution of Lys 29 with the shorter side chains of glutamine and threonine is unlikely to introduce a new interaction between residue 29 and Asp 21. The difference between glutamine and threonine at position 29 may result from indirect effects through Asn 25, which lies between residues 21 and 29 (Figures 2 and 3B), or perhaps through specific water molecules residing in or near the groove in which Asp 21 and Lys 29 are found.

The largest disagreement between observed and predicted pK_a values in ubiquitin is seen at Glu 34. However, the TK−BK model does a good job of predicting the change in pK_a at Glu 34 when Lys 11 is replaced with a neutral residue (Table 3). The pK_a for Glu 34 in wild-type ubiquitin is 4.5, very similar to model compound values, but the pK_a in K11Q and K11T is about 5.3, an unusually high pK_a for a protein carboxyl group (*38*). In the crystal structure, the carboxyl oxygen atoms in Glu 34 are the most buried of all glutamate oxygens in ubiquitin, exposing only about 30% of their maximum possible surface to solvent (Table 1; Figure 3C), so desolvation may be increasing the pK_a for Glu 34. The energetics of desolvation are not included in the TK−BK model, and the results for Glu 34 suggest that this may be a significant shortcoming. However, the carboxyl groups of Asp 21 and Asp 39 are buried to similar extents, and the predicted pK_a values for these residues agree with the experimental values (Table 1). Alternatively, the pK_a for Glu 34 may be higher than expected because neighboring positively charged groups in the crystal structure are not making the expected contribution to a positive electrostatic potential. For example, the ϵ-amino group of Lys 33 is less than 6 Å from the carboxyl group of Glu 34 in the crystal structure (Table 2; Figure 3C), but substituting Lys 33 with glutamine does not lead to the expected increase in pK_a at Glu 34 (Table 3). An alternative explanation for the high pK_a for Glu 34 is its location at the C-terminus of the helix and an unfavorable interaction with the negative end of the helix dipole (*64*−*69*). For the other mutant, K33T, we hypothesize that the surprising decrease in pK_a for Glu 34 in K33T results from a new short-range interaction, possibly a hydrogen bond, between the side chains of Thr 33 and Glu 34

The observed pK_a for Asp 52 is moderately low at 3.4 and similar to the predicted value of 3.2. In the crystal structure, Asp 52 makes a salt-bridge to Lys 27, and the carboxyl group is partially buried (Table 1). This is very reminiscent of the salt-bridge interaction between Lys 11 and Glu 34.

The pK_a of 3.8 for Glu 51 is the lowest among the glutamate residues in ubiquitin and 0.5 unit less than the lowest model compound value. The molecular basis for this relatively low glutamate pK_a is unclear. In the crystal structure, the carboxyl group of Glu 51 is well exposed to solvent. The guanidino group of Arg 54 is the nearest positively charged group, about 5.7 Å away, and the next nearest is the Lys 27 ϵ-amino group, which is 9.8 Å away. The previous observations regarding solvent-exposed carboxyl groups and the TK−BK predictions lead us to expect a pK_a for this group that is close to model compound values. However, the environment for Glu 51 varies considerably in the crystal structures of covalent dimers and tetramers of ubiquitin, with the positively charged side chains of Arg 54 and Lys 48 approaching within about 5 Å of the carboxyl group on Glu 51 (*62*, *70*). Thus, the relatively low pK_a for Glu 51 may reflect side chain conformations in solution for Arg 54 and Lys 48 that differ from those in the crystal structure of monomeric ubiquitin. However, in contrast to the case of Glu 64 discussed earlier, we are obliged to propose that the side chains for Arg 54 and Lys 48 are closer to Glu 51 in solution than in the crystal structure.

Hill Coefficients and Interactions between Carboxyl Groups. Hill coefficients for Asp 21, Glu 24, Asp 52, and, possibly, Glu 18 are significantly < 1. The Hill coefficient in eq 1 is a measure of possible interactions among titrating groups (*71*). A Hill coefficient of one reflects a monophasic titration while Hill coefficients less than or greater than one suggest that the pK_a for a carboxyl group is changing while the group is titrating. For example, a Hill coefficient < 1 suggests that the carboxyl pK_a is greater at the high-pH end of the titration than at the low-pH end. If such changes in pK_a are entirely the result of changes in electrostatic interactions with other groups titrating at acidic pH, then the most likely groups contributing to such effects are other carboxyl groups and histidine imidazole groups with low pK_a values.

The carboxyl group nearest the side chain of Asp 21 is that of Glu 18 and vice versa (Figures 2 and 3B). The carboxyl groups of Glu 24 are Asp 52 are likewise the closest to one another and separated by 5.1 Å. In principle, these close approaches are the simplest explanation for the low Hill coefficients at all four residues. However, the pK_a values for Glu 18 and Asp 21 and for Glu 24 and Asp 52 differ by about 1 unit (Table 1), so the pH transitions for these pairs of residues only overlap over about 1 pH unit (Figure 1). Nevertheless, the close approach of these carboxyl groups is the simplest hypothesis to explain the low Hill coefficients.

Carboxyl Groups and Ubiquitin Stability. The contributions of ionizable residues to the stability and the pH dependence of stability in ubiquitin have been investigated previously (*48*, *49*). At 25 °C, the stability of mammalian ubiquitin increases by about 20 kJ/mol in going from pH 2 to pH 4. This change is due to the thermodynamic linkage between protein stability and proton binding in the native and denatured states of ubiquitin (*48*): carboxyl pK_a values

that are different in the native and denatured states give rise to changes in stability with varying acid pH because these two states have different affinities for protons. If we assume that pK_a values for aspartate and glutamate in denatured ubiquitin are 4.0 and 4.5, respectively, then carboxyl pK_a values for native ubiquitin can be used to calculate the change in stability in going from pH 2 to pH 4. Stability was measured at very low ionic strength, about 0.01, while the pK_a determinations were done in the presence of 0.1 M KCl, so comparison of calculated and experimental changes in stability is somewhat tentative. Nevertheless, the calculated change is 23 kJ/mol, very similar to the change measured by calorimetry (*49*).

A previous study of yeast ubiquitin, which differs from mammalian ubiquitin by three conservative substitutions, investigated changes in stability upon substituting glutamine for lysine at position 29 (49). At pH 5 and 25 °C, K29Q is 7 kJ/mol is less stable than wild-type protein. This is consistent with disruption of the favorable electrostatic interactions of Lys 29 with Asp 21, Asp 32, and, perhaps, Glu 18 and Glu 34 observed in the present study (Table 3).

Distance Dependence of Electrostatic Interactions. The major pK_a perturbations resulting from mutations in ubiquitin involve charged groups separated by <5 Å, and no significant interactions are evident beyond separations of about 8.5 Å (Tables 2 and 3). However, proximity between lysine amino groups and carboxyl groups in the crystal structure does not guarantee a large increase in carboxyl pK_a upon mutation of the neighboring lysine residue, as evidenced by the results for K33Q (Tables 2 and 3). The results for K33Q are similar to those for Lys 34 in ovomucoid third domain, where mutation to neutral residues had no effect on the pK_a for Asp 7, despite a short 5 Å separation between the amino and carboxyl groups of these residues (*24*).

The general trend in ubiquitin is that pK_a perturbations tend to be greatest when sites of mutation are close, and this is qualitatively consistent with results from previous studies that combined mutagenesis and pK_a perturbations (*24*, *41*, *42*, and references therein). However, many of these studies identified interactions at distances exceeding 10 Å. One possible explanation for longer range interactions in previous studies is that at least one of the sites is usually buried, leading to electrostatic interactions through the low dielectric protein interior. None of the charged groups investigated in the present study of ubiquitin is completely buried. The electrostatic interactions in ubiquitin are thus dominated by the high dielectric solvent and protein−solvent interface (*29*, *33*).

CONCLUSIONS

The present study of wild-type and mutant ubiquitins has revealed much regarding the molecular basis for some of the twelve carboxyl pK_a values, particularly at six of the seven most solvent-exposed groups and Asp 21 and Glu 34. However, significant questions remain regarding these seven and, especially, the remaining four carboxyl groups. The approach combining mutagenesis and pK_a determinations is a very fruitful way to identify the role played by specific groups in modulating ionization equilibria at carboxyl groups in ubiquitin and this will be pursued further. In addition, a need for more structural information for wild-type and mutant ubiquitins is clear. For example, many of the hypotheses generated from this work invoke differences between X-ray and solution structure for wild-type ubiquitin or the introduction of new short-range interactions by mutagenesis. To partially address the latter, we have recently embarked on X-ray studies of mutants. Preliminary results are promising, and we hope to communicate results soon. However, addressing hypotheses regarding possible differences in X-ray and solution structures is going to be more challenging.

To test these hypotheses, structural information is needed for solvent-exposed side chains in solution and at different pH values. Multidimensional NMR is the best approach to determine protein conformation in solution, but in practice, determining side chain conformations at solvent-exposed residues suffers from significant uncertainties. At buried side chains, interresidue NOEs provide key information regarding side chain conformations, but few such NOEs are observed at solvent-exposed residues. Scalar and dipolar coupling constants can provide important constraints on side-chain torsion angles, but few, if any, of the available NMR experiments provide information on torsion angles beyond chi-1 (*72*, *73*). In addition, the solvent-exposed side chains are likely to be sampling multiple conformations. All of these issues represent significant technical challenges, but given the functional importance of the solvent-exposed surfaces of proteins, the need to address these challenges is compelling.

ACKNOWLEDGMENT

The authors thank Rhonda Thomas and Jared Helm for contributions to the initial stages of this study and Dr. William R. Kearney for assistance with the NMR experiments.

REFERENCES

1. Jackson, S. E., and Fersht, A. R. (1993) Contribution of long-range electrostatic interactions to the stabilization of the catalytic transition state of the serine protease subtilisin BPN′, *Biochemistry 32*, 13909−13916.
2. Honig, B., and Nicholls, A. (1995) Classical electrostatics in biology and chemistry, *Science 268*, 1144−1149.
3. Marqusee, S., and Sauer, R. T. (1994) Contributions of a hydrogen bond/salt bridge network to the stability of secondary and tertiary structure in lambda repressor, *Protein Sci. 3*, 2217−2225.
4. Pappenberger, G., Schurig, H., and Jaenicke, R. (1997) Disruption of an ionic network leads to accelerated thermal denaturation of D-glyceraldehyde-3-phosphate dehydrogenase from the hyperthermophilic bacterium Thermotoga maritima, *J. Mol. Biol. 274*, 676−683.
5. Shaw, K. L., Grimsley, G. R., Yakovlev, G. I., Makarov, A. A., and Pace, C. N. (2001) The effect of net charge on the solubility, activity, and stability of ribonuclease Sa, *Protein Sci. 10*, 1206−1215.
6. Warshel, A. (1981) Electrostatic basis of structure-function correlation in proteins, *Acc. Chem. Res. 14*, 284−290.
7. Dillet, V., Dyson, H. J., and Bashford, D. (1998) Calculations of electrostatic interactions and pK_as in the active site of Escherichia coli thioredoxin, *Biochemistry 37*, 10298−10306.
8. Beard, M. B., Olsen, A. E., Jones, R. E., Erdogan, S., Houslay, M. D., and Bolger, G. B. (2000) UCR1 and UCR2 domains unique to the cAMP-specific phosphodiesterase family form a discrete module via electrostatic interactions, *J. Biol. Chem. 275*, 10349−10358.
9. Archontis, G., Simonson, T., and Karplus, M. (2001) Binding free energies and free energy components from molecular dynamics and Poisson−Boltzmann calculations. Application to amino acid recognition by aspartyl-tRNA synthetase, *J. Mol. Biol. 306*, 307−327.

10. Thoden, J. B., Phillips, G. N., Jr., Neal, T. M., Raushel, F. M., and Holden, H. M. (2001) Molecular structure of dihydroorotase: a paradigm for catalysis through the use of a binuclear metal center, *Biochemistry 40*, 6989−6997.
11. Joshi, M. D., Sidhu, G., Nielsen, J. E., Brayer, G. D., Withers, S. G., and McIntosh, L. P. (2001) Dissecting the electrostatic interactions and pH-dependent activity of a family 11 glycosidase, *Biochemistry 40*, 10115−10139.
12. Zhang, L. Y., Gallicchio, E., Friesner, R. A., and Levy, R. M. (2001) Solvent models for protein−ligand binding: Comparison of implicit solvent Poisson and surface generalized born models with explicit solvent simulations, *J. Comput. Chem. 22*, 591−607.
13. Kangas, E., and Tidor, B. (2001) Electrostatic complementarity at ligand binding sites: Application to chorismate mutase, *J. Phys. Chem. B 105*, 880−888.
14. Rees, D. C. (1980) Experimental evaluation of the effective dielectric constant of proteins, *J. Mol. Biol. 141*, 323−326.
15. Warwicker, J. (1998) Modeling charge interactions and redox properties in DsbA, *J. Biol. Chem. 273*, 2501−2504.
16. Michel, H. (1999) Cytochrome c oxidase: catalytic cycle and mechanisms of proton pumping−a discussion, *Biochemistry 38*, 15129−15140.
17. Ebina, S., and Wüthrich, K. (1984) Amide proton titration shifts in bull seminal inhibitor IIA by two-dimensional correlated ^{1}H nuclear magnetic resonance (COSY). Manifestation of conformational equilibria involving carboxylate groups, *J. Mol. Biol. 179*, 283−288.
18. Oda, Y., Yamazaki, T., Nagayama, K., Kanaya, S., Kuroda, Y., and Nakamura, H. (1994) Individual ionization constants of all the carboxyl groups in ribonuclease HI from Escherichia coli determined by NMR, *Biochemistry 33*, 5275−5284.
19. Qin, J., Clore, G. M., and Gronenborn, A. M. (1996) Ionization equilibria for side-chain carboxyl groups in oxidized and reduced human thioredoxin and in the complex with its target peptide from the transcription factor NF kappa B, *Biochemistry 35*, 7−13.
20. Fisher, B. M., Schultz, L. W., and Raines, R. T. (1998) Coulombic effects of remote subsites on the active site of ribonuclease A, *Biochemistry 37*, 17386−17401.
21. Perez-Canadillas, J. M., Campos-Olizas, R., Lacadena, J., Martinez del Pozo, A., Gavilanes, J. G., Santoro, J., Rico, M., and Bruix, M. (1998) Characterization of pK_a values and titration shifts in the cytotoxic ribonuclease alpha-sarcin by NMR. Relationship between electrostatic interactions, structure, and catalytic function, *Biochemistry 37*, 15865−15876.
22. Kuhlman, B., Luisi, D., Young, P., and Raleigh, D. P. (1999) pK_a values and the pH dependent stability of the N-terminal domain of L9 as probes of electrostatic interactions in the denatured state. Differentiation between local and nonlocal interactions, *Biochemistry 38*, 4896−4903.
23. Forsyth, W. R., Gilson, M. K., Antosiewicz, J., Jaren, O. R., and Robertson, A. D. (1998) Theoretical and experimental analysis of ionization equilibria in ovomucoid third domain, *Biochemistry 37*, 8643−8652.
24. Forsyth, W. R., and Robertson, A. D. (2000) Insensitivity of perturbed carboxyl pK(a) values in the ovomucoid third domain to charge replacement at a neighboring residue, *Biochemistry 39*, 8067−8072.
25. Chen, H. A., Pfuhl, M., McAlister, M. S. B., and Driscoll, P. C. (2000) Determination of pK_a values of carboxyl groups in the N-terminal domain of rat CD2: anomalous pK_a of a glutamate on the ligand-binding surface, *Biochemistry 39*, 6814−6824.
26. Warshel, A., Russel, S. T., and Churg, A. K. (1984) Macroscopic models for studies of electrostatic interactions in proteins: limitations and applicability, *Proc. Natl. Acad. Sci. U.S.A. 81*, 4785−4789.
27. Bashford, D., and Karplus, M. (1991) Multiple-site titration curves of proteins − an analysis of exact and approximate methods for their calculation, *J. Phys. Chem. 95*, 9556−9561.
28. Bashford, D., Case, D. A., Dalvit, C., Tennant, L., and Wright, P. E. (1993) Electrostatic calculations of side-chain pK(a) values in myoglobin and comparison with NMR data for histidines, *Biochemistry 32*, 8045−8056.
29. Antosiewicz, J., McCammon, J. A., and Gilson, M. K. (1996) The determinants of pK_as in proteins, *Biochemistry 35*, 7819−7833.
30. Warwicker, J. (1999) Simplified methods for pK_a and acid pH-dependent stability estimation in proteins: removing dielectric and counterion boundaries, *Protein Sci. 8*, 418−425.
31. Sheinerman, F. B., Norel, R., and Honig, B. (2000) Electrostatic aspects of protein-protein interactions, *Curr. Opin. Struct. Biol. 10*, 153−159.
32. Simonson, T. (2001) Macromolecular electrostatics: continuum models and their growing pains, *Curr. Opin. Struct. Biol. 11*, 243−252.
33. Schutz, C. N., and Warshel, A. (2001) What are the dielectric "constants" of proteins and how to validate electrostatic models?, *Proteins 44*, 400−417.
34. Tanford, C., and Kirkwood, J. G. (1957) Theory of protein titration curves. I. General equations for impenetrable spheres, *J. Am. Chem. Soc. 79*, 5333−5339.
35. Warshel, A., and Russell, S. (1984) Calculations of electrostatic interactions in biological systems and in solutions, *Q. Rev. Biophys. 17*, 283−422.
36. Havranek, J. J., and Harbury, P. H. (1999) Tanford-Kirkwood electrostatics for protein modeling, *Proc. Natl. Acad. Sci. U.S.A. 96*, 11145−11150.
37. Kao, Y.-H., Fitch, C. A., Bhattacharya, S., Sarkisian, C. J., Lecomte, J. T. J., and Garcia-Moreno E., B. (2000) Salt effects on ionization equilibria of histidines in myoglobin, *Biophys. J. 79*, 1637−1654.
38. Forsyth, W. R., Antosiewicz, J. M., and Robertson, A. D. (2002) Empirical relationships between protein structure and carboxyl pK_a values in proteins, *Proteins*, in press.
39. Edgcomb, S. P., and Murphy, K. P. (2002) Variability in the pK_a of histidine side-chains correlates with burial within proteins, *Proteins*, in press.
40. Dwyer, J. J., Gittis, A. G., Karp, D. A., Lattman, E. E., Spencer, D. S., Stites, W. E., and Garcia-Moreno, E., B. (2000) High apparent dielectric constants in the interior of a protein reflect water penetration, *Biophys. J. 79*, 1610−1620.
41. Tishmack, P. A., Bashford, D., Harms, E., and Van Etten, R. L. (1997) Use of ^{1}H NMR spectroscopy and computer simulations to analyze histidine pK_a changes in a protein tyrosine phosphatase: experimental and theoretical determination of electrostatic properties in a small protein, *Biochemistry 36*, 11984−11994.
42. Lee, K. K., Fitch, C. A., Garcia-Moreno E., B. (2002) Distance dependence and salt sensitivity of pairwise coulombic interactions in a protein, *Protein Sci. 11*, 1004−1016.
43. Vijay-Kumar, S., Bugg, C. E., and Cook, W. J. (1987) Struture at ubiquitin refined at 1.8 A resolution, *J. Mol. Biol. 194*, 531−544.
44. Wintrode, P. L., Makhatadze, G. I., and Privalov, P. L. (1994) Thermodynamics of ubiquitin unfolding, *Proteins 18*, 246−253.
45. Sivaraman, T., Arrington, C. B., and Robertson, A. D. (2001) Kinetics of unfolding and folding from amide hydrogen exchange in native ubiquitin, *Nat. Struct. Biol. 8*, 331−333.
46. Di Stefano, D. L., and Wand, A. J. (1987) Two-dimensional ^{1}H NMR study of human ubiquitin: a main chain directed assignment and structure analysis, *Biochemistry 26*, 7272−7281.
47. Weber, P. L., Brown, S. C., and Mueller, L. (1987) Sequential ^{1}H NMR assignments and secondary structure identification of human ubiquitin, *Biochemistry 26*, 7282−7290.
48. Ibarra-Molero, B., Loladze, V. V., Makhatadze, G. I., and Sanchez-Ruiz, J. M. (1999) Thermal versus guanidine-induced unfolding of ubiquitin. An analysis in terms of the contributions from charge−charge interactions to protein stability, *Biochemistry 38*, 8138−8149.
49. Loladze, V. V., Ibarra-Molero, B., Sanchez-Ruiz, J. M., and Makhatadze, G. I. (1999) Engineering a thermostable protein via optimization of charge−charge interactions on the protein surface, *Biochemistry 38*, 16419−16423.
50. Loladze, V. V., and Makhatadze, G. I. (2002) Removal of surface charge−charge interactions from ubiquitin leaves the protein folded and very stable, *Protein Sci. 11*, 174−177.
51. Shire, S., Hanania, G. I. H., and Gurd, F. R. N. (1974) Electrostatic effects in myoglobin. Hydrogen ion equilibria in sperm whale ferrimyoglobin, *Biochemistry 13*, 2967−2974.
52. Matthew, J. B., and Gurd, F. R. N. (1986) Calculation of electrostatic interactions in proteins, *Methods Enzymol. 130*, 413−453.
53. Piotrowski, J., Beal, R., Hoffman, L., Wilkinson, K. D., Cohen, R. E., and Pickart, C. M. (1997) Inhibition of the 26 S proteasome by polyubiquitin chains synthesized to have defined lengths, *J. Biol. Chem. 272*, 23712−23721.
54. Bax, A. (1989) Homonuclear Hartmann−Hahn experiments, *Methods Enzymol. 176*, 151−168.

55. Van Geet, A. L. (1968) Calibration of the methanol and glycol nuclear magnetic resonance thermometers with a static thermistor probe, *Anal. Chem. 40*, 2227−2229.
56. DeMarco, A. (1977) pH dependence of internal references, *J. Magn. Reson. 26*, 527−528.
57. Bundi, A., and Wüthrich, K. (1979) ^{1}H NMR parameters of the common amino acid residues measured in aqueous solutions of the linear tetrapeptides H-Gly-Gly-X-L-Ala-OH, *Biopolymers 18*, 285−297.
58. Wishart, D. S., and Case, D. A. (2001) Use of chemical shifts in macromolecular structure determination, *Methods Enzymol. 338*, 3−34.
59. Khorasanizadeh, S., Peters, I. D., Butt, T. R., and Roder, H. (1993) Folding and stability of a tryptophan-containing mutant of ubiquitin, *Biochemistry 32*, 7054−7063.
60. Bundi, A., and Wüthrich, K. (1979) Use of amide ^{1}H NMR titration shifts for studies of polypeptide conformation, *Biopolymers 18*, 299−311.
61. Mayer, R., Lancelot, G., and Spach, G. (1979) Side chain-backbone hydrogen bonds in peptides containing glutamic acid residues, *Biopolymers 18*, 1293−1295.
62. Phillips, C. L., Thrower, J., Pickart, C. M., and Hill, C. P. (2001) Structure of a new crystal form of tetraubiquitin, *Acta Crystallogr., Sect. D 57*, 341−344.
63. Creighton, T. E. (1993) *Proteins: Structure and Molecular Properties* 2nd ed., W. H. Freeman and Company, New York.
64. Wada, A. (1976) The alpha-helix as an electric macro-dipole, *Adv. Biophys. 9*, 1−63.
65. Hol, W. G. J. (1985) The role of the alpha-helix dipole in protein function and structure, *Prog. Biophys. Mol. Biol. 45*, 149−195.
66. Nicholson, H., Anderson, D. E., Dao-pin, S., and Matthews, B. W. (1991) Analysis of the interaction between charged side chains and the alpha-helix dipole using designed thermostable mutants of phage T4 lysozyme, *Biochemistry 30*, 9816−9828.
67. Sancho, J., Serrano, L., and Fersht, A. R. (1992) Histidine residues at the N- and C-termini of alpha-helices: perturbed pK_as and protein stability, *Biochemistry 31*, 2253−2258.
68. Lockhart, D. J., and Kim, P. S. (1993) Electrostatic screening of charge and dipole interactions with the helix backbone, *Science 260*, 198−202.
69. Kortemme, T., and Creighton, T. E. (1995) Ionisation of cysteine residues at the termini of model alpha-helical peptides. Relevance to unusual thiol pK_a values in proteins of the thioredoxin family, *J. Mol. Biol. 253*, 799−812.
70. Cook, W. J., Jeffrey, L. C., Carson, M., Chen, Z., and Pickart, C. M. (1992) Structure of a diubiquitin conjugate and a model for interaction with ubiquitin conjugating enzyme (E2), *J. Biol. Chem. 267*, 16467−16471.
71. Markley, J. L. (1975) Observation of histidine residues in proteins by means of nuclear magnetic resonance spectroscopy, *Acc. Chem. Res. 8*, 70−80.
72. Ferentz, A. E., and Wagner, G. (2000) NMR spectroscopy: a multifaceted approach to macromolecular structure, *Q. Rev. Biophys. 33*, 29−65.
73. Bax, A., Kontaxis, G., and Tjandra, N. (2001) Dipolar couplings in macromolecular structure determination, *Methods Enzymol. 339*, 127−174.
74. Vriend, G. (1990) WHAT IF - A moleclar modeling and drug design program, *J. Mol. Graph. 8*, 52−56.

BI025571D